Finite element modeling of an energy storing and return prosthetic foot and implications of stiffness on rollover shape

Journal Title
XX(X):2–18

DOI: 10.1177/ToBeAssigned
www.sagepub.com/
SAGE

Finite element modeling of an energy storing and return prosthetic foot and implications of stiffness on rollover shape

Lorenzo Cavallaro[2], Federico Tessari[1,2], Giovanni Milandri[2], Carlo De Benedictis[1], Carlo Ferraresi[1], Matteo Laffranchi[2] and Lorenzo De Michieli[2]

Abstract

Energy storing and return (ESAR) prosthetic feet showed continuous improvements during the last 30 years. Despite this, standard guidelines are still missing to achieve an optimal foot design in terms of performances. One of the most important design parameters in ESAR feet is the Rollover Shape (RoS). This represents the foot Center of Pressure (CoP) path in a shank-based coordinate system during stance. RoS objectively describes the foot behavior according to its stiffness, which depends on foot geometry and material. This work presents the development of a finite element modeling methodology able to predict the stiffness characteristic of an ESAR foot and its RoS. The validation of the model is performed on a well-known commercially available prosthetic foot both in bench tests and realistic walking scenario. The obtained results confirm an error of +6.1% on stiffness estimation and +10.2% on RoS evaluation, which underlines that the proposed method is a powerful tool able to replicate the mechanical behavior of a prosthetic foot.

Keywords

Prosthetic Foot, Finite Element Analysis, Foot Stiffness, Rollover Shape

Prepared using sagej.cls *[Version: 2017/01/17 v1.20]*

Introduction

Over the past thirty years, prosthetic foot technology has witnessed the design, evolution and improvement of different passive and active devices. The development of such prostheses is mainly oriented to mitigate foot impact, to provide stability during gait, to control weight transfer from heel to toe during stance phase and, finally, to store and return energy during propulsion phase.[1]

The main mechanical characteristic of a passive prosthetic foot is its stiffness, which results from the combination of implemented geometry and material properties, and defines foot deformation and energy stored and returned to the patient during the gait cycle. Prosthetic feet achieve the desired stiffness characteristic with two main architectures. The first consists in utilizing an independent blade design, thus decoupling the deformation of heel and toe in two different components (as it occurs in the Echelon (Blatchford Ltd., Basingstoke, UK) or Renegade (Freedom Innovations LLC, Irvine, CA, USA) prosthetic feet). The second, instead, utilizes two joined blades, each interacting in a specific portion of the gait cycle, e.g. the Variflex foot ($\ddot{O}ssur$, hf., Reykjavik, Iceland). While desired stiffness can be designed with both solutions, the latter is more advantageous with respect to the first for two reasons. The first is the possibility of keeping relatively low thickness blades while achieving a non-linear stiffness profile through the interaction of both components simultaneously. The second is the possibility of maximizing the energy restitution throughout the design of the keel while remaining in the anthropometric volume of the human foot, since heel blade bulkiness is reduced. For these reasons, it has been decided to focus the investigation on a Variflex-like foot design.

Effects of the stiffness profile on prosthesis performances have been the focus of different studies[2–5]. A decrease in stiffness of prosthetic feet is considered responsible for higher ground reaction force (GRF) and muscle activity on the residual limb during mid-stance.[6] Lowering forefoot stiffness improves mechanical efficiency and energy storage and return, while higher stiffness increases patient comfort and reduce the prosthetic limb motor work over the center of mass.[2,7,8] Moreover, increased stiffness in the hind-foot can provide a lower energy restitution, higher knee flexion angle during stance and knee extension during mid-stance, but also causes higher inter-articular forces in the sound limb during heel strike.[4] Despite these findings, different issues remain unsolved, e.g. the lack of comfort of different prostheses, the prevalence of osteoarthritis in the amputee intact knee (due to an increased knee external abduction moment) and a general increase in the metabolic cost caused by compensatory muscle activity during gait. All these problems show that current solutions are still sub-optimal, especially in the long term.[9–11]

[1]Department of Mechanical and Aerospace Engineering, DIMEAS, Politecnico di Torino, Corso Duca degli Abruzzi, 24, Turin, Italy
[2]Rehab Technologies, Italian Institute of Technolog, Via Morego,30, Genova, Italy

Corresponding author:
Federico Tessari, Via Morego 30, Genova, Italy, 16163
Email: federico.tessari@iit.it

Prepared using sagej.cls

Nowadays, design specifications for achieving an optimal Energy Storage and Return (ESAR) foot are still missing. Moreover, the lack of standardized methods for the evaluation of prosthetic feet energy behavior can lead to misclassifications, thus complicating the comparison among the available prostheses. A solution to this problem has been proposed by Hafner *et al.*[12]. In their work, they suggest a renewed nomenclature and emphasize the importance of keel and heel energy contribution to the overall prosthesis performances. It is critical to correlate patient perception of the foot to its mechanical properties, as Hafner *et al.*[13] summarized in their review. The international standards ISO 10328 and 22675 are mainly focused on the strength and longevity of the product and not on its performance when utilized by a patient. The American Orthotic & Prosthetic Association (AOPA) developed a series of tests with some target values for foot characterization to help in prosthetic design, but they still rely on a trial and error approach which results in a major innovation barrier due to prototyping costs, especially for smaller companies. Moreover, even prosthetic feet that are not appreciated by patients and therapists, e.g. too stiff, bad heel impact response, etc., can satisfy ISO standards.

In this scenario, Rollover Shape can be considered a fundamental feature to evaluate prosthetic feet performance. It represents the path of the Center of Pressure (CoP) of a foot as seen from a local coordinate system integral with the shank. It is typically fitted with a circle. The radius and the anteriority of its center with respect to the origin in the sagittal plane are the parameters considered in the RoS computation (anteriority is considered as the positive or anterior - namely towards the toe - distance between the RoS center of the fitting circular arc and the shank-based coordinate system origin). Among the three rollover-shape systems identified in the literature[20], the knee-ankle-foot (KAF) and the ankle-foot (AF) ones are the most interesting regarding lower limb prosthesis design. While the former is capable of including the overall behaviour of the lower limb during gait, the latter gives a better quantitative representation of the combination of foot stiffness and shape, without considering the knee contribution (which can, in fact, change depending on the prosthesis type and user capability).Therefore AF RoS system parameters are an interesting foundation for prosthetic foot evaluation (as suggested by Hansen *et al.*[20]), where the origin of the system is considered approximately at the ankle joint location. It has been found that, in an healthy physiological gait, the fitted circle radius is about 0.3 ± 0.1 times the leg length. This radius tends to be independent of carried weights, walking speeds or heel heights[21]. This is due to the individual ability to adapt to different ground or load conditions and thus, to maintain the RoS radius invariant. Adamczyk *et al*. conducted evaluation of RoS in healthy subjects[22,23]; they found interesting association between RoS values and their effect on center of mass (CoM) work reduction, especially in step-to-step transitions. The RoS radius in prosthetic feet seems to follow the same principle, where popular prosthetic feet tend to have a radius value similar to physiological ones[24]. This is true for level walking, while some changes in the RoS profile have been highlighted by Hansen *et al.*[21]. Their study reflected the RoS adaptation of able-bodied ankle joint behavior to different scenarios such as slopes and stairs. Micro-processor-based prosthetic devices (such as the Elan foot) provide self-alignment capabilities, which can improve walking and standing effort[25,26]. This is not possible for ESAR feet

that rely on pure deformation of the blades, thus resulting in a higher load on the sound limb with consequent increased effort required by the amputee.

Since the stiffness characteristics determines the deformation of the foot throughout the gait cycle, and being the RoS a representation of the deformed profile under the same load conditions, then RoS can stand as a reasonable parameter for foot design. For example, it can be used to discard possible designs that would produce prosthetic feet with a radius that exceeds the aforementioned physiological values.

In order to reduce the number of prototypes needed at the design stage, Finite Element Analysis (FEA) represents a powerful tool that can be used to evaluate the performance of a component, e.g. a prosthetic foot. This aspect is particularly significant in the manufacturing of prostheses, sine it might help reducing the overall design time and cost. Even if different works on FEA applied to prosthetic feet can be found in literature, only few of these works include ESAR feet[14–16]. Moreover, most of them are focused on stress-strain investigations under ISO 10328 conditions, as in Bonnet *et al.*[17] Among the most recent works, Song *et al.*[18] replicated the Vari-Flex LP ($\ddot{O}ssur$) properties, optimizing its geometry for lowering production costs. In addition, Tryggvason *et al.* collaborated with $\ddot{O}ssur$ for an ankle joint design optimization of their Pro-Flex prosthetic foot[19].

A simplified approach that included a RoS evaluation was proposed by Mahmoodi *et al.*[27], where the concept of rollover is associated to a theoretical model and applied for prosthetic design optimization. Recently, Balaramakrishnan *et al.* presented a non-linear finite-element methodology to estimate the roll-over shape of a solid ankle and cushion heel (SACH) foot, with a particular focus on the foot shell, highlighting the advantages of their solution compared to standard trial-and-error approaches[28]. Combining FEA capabilities with proper parameters, such as the aforementioned RoS center and radius, would allow designers to establish the quality of a given design and to increase the efficiency of the process, that would otherwise require expensive labor and costly trial and error procedures through prototyping.

In light of these considerations, the goal of the authors is to demonstrate the validity of FEA to predict stiffness and RoS behavior of an ESAR prosthetic foot under vertical ISO-compliant load and in gait-scenario, and to provide the scientific and industrial community with a patient-independent tool able to perform early-stage design optimization of new prosthetic feet.

The paper is structured as follows: the Methodology section presents the approach adopted for the mechanical testing of a commercial prosthetic foot and for the development of a finite element model of the foot. The Results section shows the outcome of both experimental trials and simulations, subsequently commented in the Discussion section. The Conclusion section summarizes the achieved results and presents the future developments of this research.

Methodology

The prosthesis analyzed and used as a reference for the application and validation of the presented methodology is a Vari-Flex (CAT 6 - L 27) by $\ddot{O}ssur$. It is an ESAR carbon fiber prosthetic foot widely used by the amputee community which is composed of heel medial and lateral blades bolted to a split keel in the midfoot, and with a carbon

tube as a means of connection to the pylon. Two feet of the same size and category were analyzed, one for material investigation including destructive test, the other for stiffness investigation. This was achieved with 2 different test campaigns: a *Single Component Test* session, following an internal protocol, was conducted to extract material properties, while a *Foot Compression Test* based on ISO 22675 guidelines was carried out for FEA validation. It has been proven that ISO 22675 fatigue test is representative of a prosthetic gait force/shank angle behavior[29]. It should be noted that, in this context, the load profile should be scaled to the specific patient's weight. Moreover, no anthero-posterior GRF component is modeled in the fatigue test, which would be important for propulsion investigation. Indeed, in this case, it can be omitted since it is not among the goals of the presented work. An experimental test (*Stance Phase Analysis*) employing an able-bodied adaptor was conducted to investigate the FEA model in a realistic scenario.

FEA Model Development

The geometry of the foot was obtained by a combination of direct measurements and photogrammetry. Pictures were taken for both heel and keel components and processed in Agisoft Photoscan, then the obtained scanned model was imported in Solidworks 2018 to scale it according to actual prosthesis size. The error of the reconstructed model was analyzed by sampling several dimensions along the sagittal (namely the foot thickness) and frontal (width, height and length) profiles of the foot. Reconstruction artifacts were found on the model borders due to triangulation approximation on hard edge transitions. Such errors were compensated in SolidWorks, thus obtaining a clean model to be imported in Ansys. The overall reconstructed model showed an error of less than 1 mm.

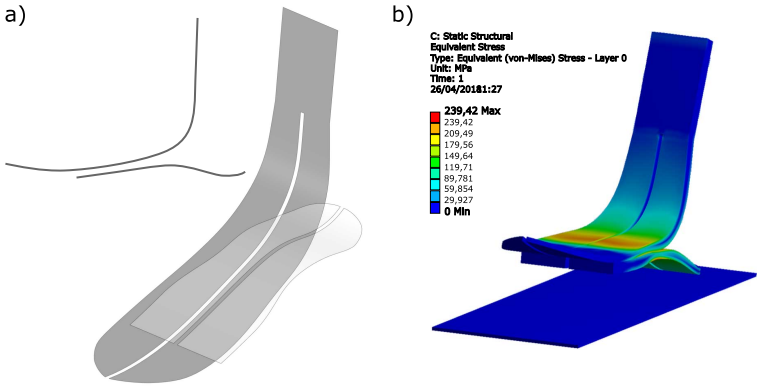

Figure 1. Vari-Flex photogrammetry profiles (a); FEA model in simulation environment (b).

The model was then exported to ANSYS Workbench, where ACP PrePost package was used for composite material modeling. In order to achieve a correctly-built model of keel and heel, each upper and lower surface was extracted in DesignModeler, the former to act as sources for composite extrusion, the latter used to apply the tapering of the carbon plies and limiting the extrusion. In ACP, the rosettes — the local coordinate

systems representing the direction of each carbon ply — were defined according to keel and heel geometry. The x-axis is always aligned with the fiber main orientation, the y-axis is in-plane perpendicular to the x-axis, and the z-axis completes the reference frame according to the right-hand rule.

Surface meshing techniques have been implemented for achieving hexagonal elements for both keel and heel components. A preliminary convergence study was conducted in order to choose the minimum element size, which was set to 4 mm maximum: smaller elements were created only if imposed by geometry and achieved throughout local mesh refinement. With a bigger mesh size, the contact region between keel and heel suffered from sudden changes in contact status, leading to different results in the overall evaluation. The number of elements was halved using symmetry condition, which resulted in simulation times ranging from 9 to 22 minutes depending on the number of contact elements. Figure 1 shows the photogrammetry profiles and the resulting model.

A carbon fiber sandwich structure was identified by means of microscopic analysis on a sample of the foot material. The core section was made of unidirectional (UD) tapered plies along the longitudinal direction of the foot (0°) and woven plies at the extremities. Some 90° UD plies were also found near the external surfaces. Following the previous considerations, each ply was modeled as an orthotropic equivalent material with thickness of 0.2 mm and UD properties. Specifically, the Young's Modulus along the x-axis (E_x) for each component was computed through direct optimization of the stiffness profile obtained in the relative *Single Lamina Test*. E_y, E_z, shear moduli and Poisson's coefficients were set using typical values of commercially available plies. Details of the carbon laminae and connection between the components are highlighted in Figure 2.

Moreover, residual pieces of a rubber wedge were found between heel and keel: this affected the stiffness profile during the *Foot Compression Test*. Wedges are usually implemented to increase foot stiffness from heel strike to flat-foot condition by shortening the lever arm of the heel. The importance of wedge in prosthetic foot response has been highlighted by Womac *et al.*[30], where up to 40% stiffness increment can be achieved with different wedges. This aspect has been investigated in the simulation by offsetting the wedge region of 1 mm.

ANSYS Static Structural node was used for the definition of contacts, load cases and boundary conditions to replicate the experimental setup. The foot was clamped with a *Fixed Support* constraint in the upper bolted region, oriented according to ISO 22675 protocol: five key-points were chosen, each one corresponding to a specific force value and shank angle with respect to the ground, as can be seen in Figure 3. Despite prosthetic feet are almost never perfectly aligned in the frontal plane, the orientation of the foot was altered only in the sagittal plane: this allows to simplify the experimental protocol (in agreement with ISO 22675) and to avoid undesired effects from an everted alignment which would be necessary to replicate in the mechanical tests.

The first two key-points refer to the heel contact and weight acceptance phases of gait, the third coincides with flat foot condition, while the last two refer to late stance and pre-swing phases. The last position did not strictly respect ISO standards due to safety protocol in the testing laboratory. A rigid plate was modeled as close as possible to the bottom of the foot to facilitate contact recognition. It was constrained

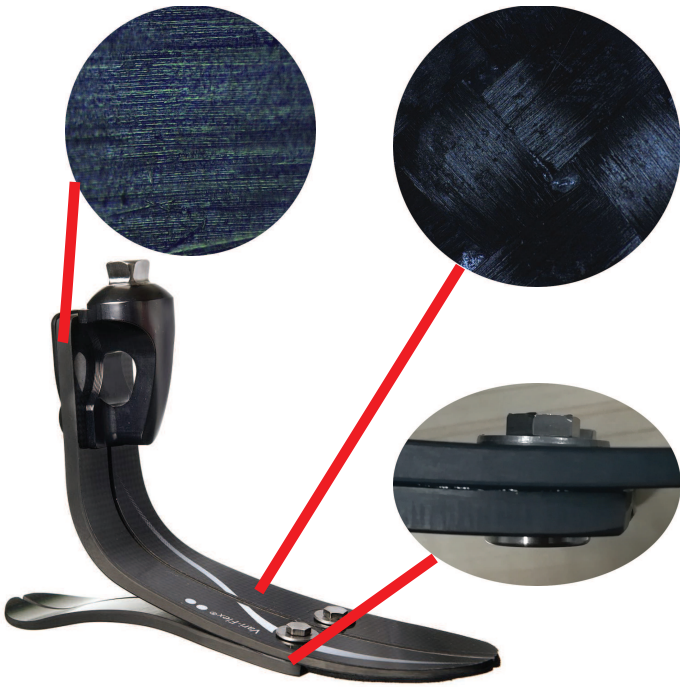

Figure 2. UD plies are stacked to give the correct thickness of the foot (top left corner); the external surfaces are made of woven carbon plies; the connection between keel and heel is achieved throughout bolts and industrial glue (bottom right corner)

to move only along the plate normal direction and a rigid displacement was imposed accordingly. This motion led to the plate-foot contact and, thus, to the generation of the relative reaction force. Foot/Plate and Keel/Heel contact regions were modeled as a friction-less non-linear type with an Augmented Lagrange formulation and default normal stiffness. Negligible differences were found switching from Asymmetric to Symmetric behavior. Contact detection was kept to Nodal – Normal Contact because of the smooth contact surfaces of the geometries. The bolted region between keel and heel was defined as a squared area of 625 mm^2, measured directly from the prosthesis, and modeled as *Bonded* surfaces with multi-point constraint (*MPC*) formulation to achieve no penetration.

Sensitivity Analysis

A sensitivity analysis was also performed to investigate the effects of the most important parameters on the foot behavior, since their variations could affect the stiffness behavior and, therefore, the overall reliability of the proposed methodology. The chosen parameters were: the Young's Modulus E_x value derived from the Single Component Test, and the contact area between heel and keel. In order to better understand the effect of such variations, the heel compression trial at 10° was chosen as sample. This was selected to include both keel and heel contribution to the

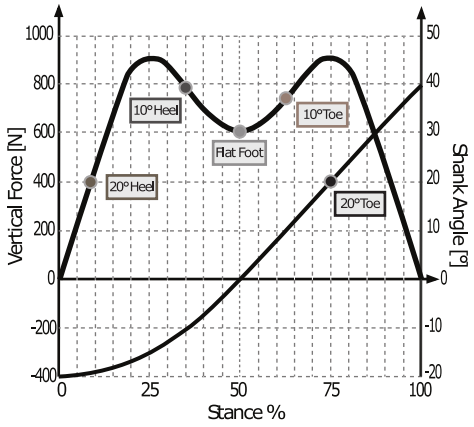

Figure 3. Key-points extracted from ISO 22675 load profile. *20° Toe* trial was set at a lower force value with respect to the actual test due to safety protocols of the testing laboratory.

overall stiffness of the prosthesis. Variation of the E_x for keel and heel components, individually and combined, were set at $\pm 20\%$ to account for model and material uncertainties. In addition, the border of the area defining contact between keel and heel were extended/reduced along the fiber direction by ± 10 mm (this represents 40% of the original region and about 3.8% of the foot total length).

Mechanical Testing

Mechanical tests were performed in order to obtain stiffness profiles of the individual laminae and of the assembled foot in different conditions. Stiffness was calculated by means of first order differentiation of force with respect to displacement, given the data extracted at each trial.

Single Component Test In order to investigate the mechanical properties of the material, a single component test campaign was carried to provide experimental data to compare with the direct optimization output of the E_x Young Modulus. Keel and heel laminae were disassembled and separately clamped in the bolted region to a fixed support: since the keel component presents two fastener sites, the upper (or proximal) bolted region was chosen. An increasing vertical load up to 15 N was applied and the vertical displacement recorded with a digital dial gauge. The definition of the load was based on laboratory equipment capabilities and considered sufficient to the goal. The load was applied at the opposite side of the clamp, 15 mm from the outermost point for the heel, 32 mm for the keel. Each trial was repeated 4 times to check for repeatability of the tests and only negligible variations were observed.

Foot Compression Test A set of compression tests based on the ISO 22675 fatigue test (Figure 3) for prosthetic feet were performed: 5 orientations (plantarflexion/dorsiflexion angle) were chosen, each one corresponding to a specific vertical load.

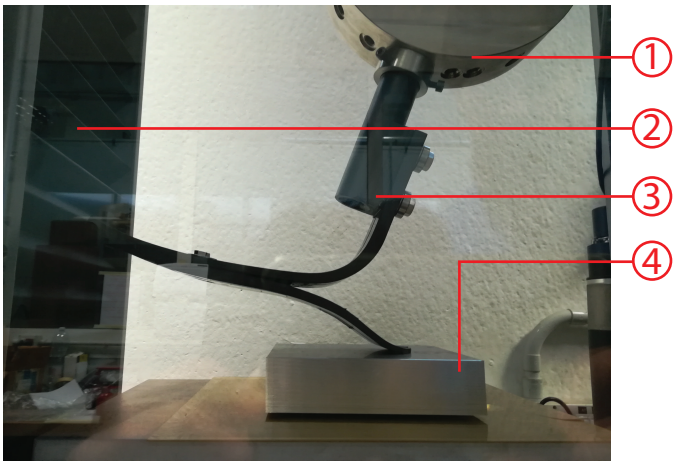

Figure 4. The overall testing environment: (1) angular adapter, (2) tensile – compression machine, (3) VariFlex Foot and (4) base plate with rolling pins for frictionless contact

A Zwick Roell tensile–compression machine, including a linear actuator, a single axis load cell and a displacement sensor, was utilized for the experimental characterizations. Load was applied at constant 5 mm/s speed. An angle adapter has been manufactured to control the prosthesis plantar and dorsi-flexion angle during each trial. This adapter was sufficiently rigid to avoid relative motion between the foot connection and the load cell. It consists of an half-moon shaped metal component with threaded holes, capable of covering all ISO 22675 with a 10° angle span. A threaded cylinder is screwed at the desired hole, having the opposite side coupled to the carbon tube of the prosthesis: in this way, a rigid connection is achieved. The foot was pushed against a metal plate with rollers beneath it to minimize friction. Figure 4 shows the described test environment. Each load case was repeated with a minimum of 5 trials for repeatability purposes. A second test session was performed on a different date, in order to account for some eventual setup errors.

Stance Phase Analysis

The stance phase analysis was performed on a healthy subject utilizing a custom-made able-bodied adapter (see Figure 5). The able-bodied adapter was connected to a prosthetic knee that was in turn coupled to the ESAR foot of interest. It is important to underline that no foot shell was introduced in this analysis. This was done to correctly compare the experimental results with FEA simulations and to avoid the introduction of undesired dynamics related to footwear. A commercial Vicon motion capture system was used to reproduce the prosthetic stance phase. The overall mass of the subject, including the adapter and the prosthesis, was of 76 kg. A raised platform shoe has been used to compensate the height difference between the sound and prosthetic limb. The alignment was checked following prosthesist guidelines, with the knee center of

rotation 22 mm posterior to the load line. This condition prevented the knee from flexing during prosthesis loading. A training session was performed to allow the user to achieve a natural heel strike angle and to properly load the prosthesis. Four reflective markers were put on the foot to identify a local coordinate system centered in the proximal bolt marker, as shown in Figure 5. Markers placed on the bolts were also used to track the angle between pylon and the ground during the trial while an AMTI force platform was used to obtain CoP location and GRFs. A Body-Builder model was used to compute synchronized CoP coordinates (in the global coordinate system), RoS coordinates (in the shank coordinate system), shank angle and the vertical GRF (GRF_z) for simulation purposes. In order to maintain the alignment between the model and the actual test scenario, two markers were placed to extract the time-shank angle relationship during stance phase trial. In the FEA model, the foot was aligned in the same configuration, so that the angle imposed matched the shank angle obtained from the Vicon system. GRF_x and GRF_y components were not implemented in the FEA model. Their lower intensity (less than 25% of GRF_z maximum value) as well as higher foot stiffness in those directions gave a negligible contribution to the foot deformation.

Figure 5. Test setup for ROS calculation - on the left, the healthy subject fitted with the able-bodied adapter; on the right, a sideview with the markerset highlited. Axes of the local coordinate system (shank) are shown

The shank angle was chosen in order to mimic ISO 22675 cyclic test profile while avoiding flexion of the knee (not included in the FEA model). Assuming that the shank perpendicular to the ground corresponds to an angle of 0° , and positive angles represent clockwise rotations, a single trial ranged from -20° up to 15°. Hip extension

was therefore provided to prevent knee flexion while performing roll-over on the foot. Among the tested trials, authors discarded those presenting: insufficient shank angle, bad load condition (not enough weight on the prosthesis) or stumbling. A custom MATLAB script was used to post-process the experimental data and compute the best-fit circle for RoS parameters estimation.

Results

Single Component Test

The stiffness value at maximum deflection is 65.2 N/mm for heel component and 41.7 N/mm for keel. Linear regression of experimental data was performed, with R^2= 0.99. Direct optimization of E_x of the carbon ply in simulation environment led to $E_x = 51000$ MPa for the heel, with an error of -8.3% on maximum stiffness, and $E_x = 38000$ MPa for the keel, where the error on stiffness is -6.5%.

Foot Compression Test

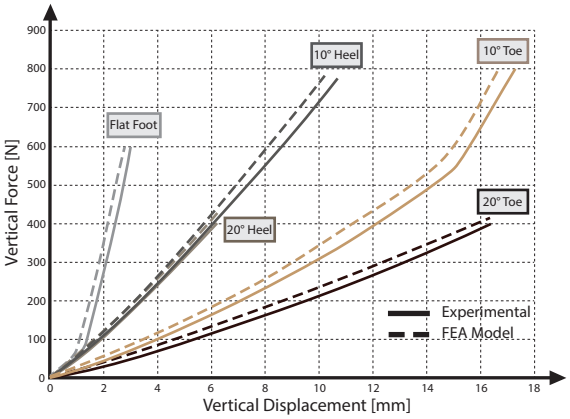

Figure 6. Comparison of experimental (solid line) and FEA (dashed line) data of the Foot Compression Test. Trial force and shank values can be extracted from the labeled point in Figure 3.

Figure 6 reports the data from the *Foot Compression Test*. The experimental results show a non-linear behavior when both keel and heel are engaged during the compression. This is more appreciable during heel compression configurations, in the shank angle range comprised within -20° and -10° . The 10° toe trial is characterized by a rapid increase of stiffness due to the contact between the plate and the bolted region of the foot. The experimental results of Figure 6 represent the average trends of the five trials performed for each configuration (see the Methodology section details). The experiments presented a high repeatability with negligible variations. In the worst case scenario, namely the 10° toe trail (strong non-linearity), the following standard deviations were observed: $STD_{pos_{max}} = \pm 0.029$ mm, $STD_{pos_{mean}} = \pm 0.007$ mm, $STD_{force_{max}} = \pm 3.4$ N, $STD_{force_{mean}} = \pm 1.25$

N. The maximum standard deviation represents the highest standard deviation measured over the experimental trend, while the mean standard deviation accounts for the average of the standard deviations computed for each point of the considered trial.

Table 1 shows the percentage error for each angular position plus the experimental stiffness value obtained as displacement-force ratio at the maximum compression condition. The authors attribute the overestimation of stiffness to the contact definition between heel and keel. In the real foot, the contact region between heel and keel is obtained by the combination of a bolted connection with additional industrial CF specific adhesive. This contact is indeed different from the one used in the FEA model (fixed bonded area), which is more rigid and affects the non-linear interaction of the blades in the neighboring region. Nonetheless, the error (+6.1 % in a single configuration) was considered acceptable for preliminary analysis of a design evaluation. The sensitivity analysis explored also this aspect of the FEA model.

Trial	Experimental Stiffness [N/mm]	FEA model Stiffness [N/mm]	Error
20° Heel	65.5	68.3	+4.2 %
10° Heel	69.3	73.5	+6.1 %
Flat Foot	213.3	218.2	+2.3 %
10° Toe	46.5	48.1	+3.5 %
20° Toe	24.4	25.7	+5.3 %

Table 1. Percentage error between experimental value and related FEA model. Stiffness values refers to maximum vertical deflection condition of the foot.

Sensitivity Analysis

The results of the sensitivity analysis are presented in Table 2. Starting from the nominal profile of the validated FEA model, the left and right colored bars represent respectively the negative and positive variations on the foot stiffness due to the analyzed parameters.

Stance Phase Analysis

The gray point cloud shown in Figure 7 shows the RoS coordinates - in the sagittal plane - obtained from experimental tests and represented in the shank-based coordinate system. The red circles represent the simulated data (obtained through FEA analysis)

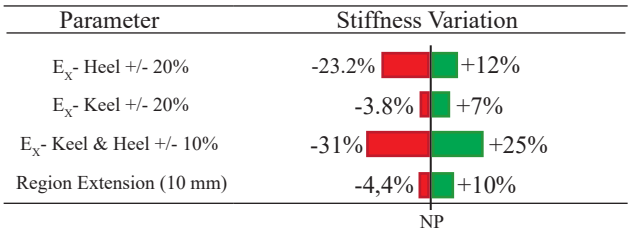

Table 2. Sensitivity Analysis of the FEA model stiffness variation. Left bars indicate a negative variation with respect to the nominal profile (NP), right bars a positive variation.

with equivalent loading conditions at different shank angles. Specifically, the red points from left to right refer to -15°,-10°,-8°,-5°,-2°,0°,+5°,+8°,+10°, respectively.

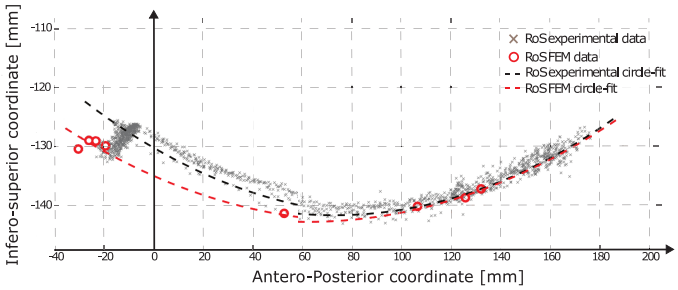

Figure 7. Point cloud showing ROS data from Vicon Setup. Red circles represents FEA point, red line is the average circumference which fits FEA data; black dashed curve is the average circular arc of the experimental data

The black dotted line is the mean circle fit of the experimental point cloud, while red dotted line represents the circle fit of FEA data. RoS radius from average experimental data is 408.7 mm, while 455 mm is the simulated one, with a difference of +10.2%. Anteriority shows an error of -11.4%, with an experimental value of 93.56 mm and 82.9 mm in simulation environment.

Discussion

The presented work showed how an equivalent FEA model is able to predict the stiffness behavior of a carbon fiber prosthetic foot. The authors believe that this model can contribute to the future development of prosthetic feet thanks to its simple load scenario, relatively fast simulation times and reliable model results. The general behavior of the stiffness is well reproduced, and the maximum error is +6.1%, similar to what is reported in the literature[17], where the ESAR foot specifications were provided by the manufacturer. No CoP imposition was performed, allowing the interaction between foot and plate to determine its location. The current implementation of an equivalent material for simulation purposes is useful as it provides suggestions for an actual design. The approximation of the material properties is a crucial portion of the presented work and implies some consequences, which were partially addressed in the sensitivity analysis. However, the approximation regarding the material properties represented also a compulsory choice since no relevant information were found in the literature. In fact, the main purpose of the microscopic analysis and of the single lamina tests was to limit the sources of error related to the modeling of the material. Such tests helped in the implementation of UD plies in terms of thickness and main Young's Modulus value (E_x). Moreover, these tests also supported the choice of standard E_y and E_z values, whose contribution was minor to the prosthesis deformation.

The performed investigations highlight important aspects of j-shaped feet. First, the non-linear stiffness profile - visible in Figure 6 -, is mainly caused by the lever arm

between the CoP location and the closest heel section in contact with the keel. Since the two blades shift their contact region during heel compression, the lever arm of the reaction force is reduced, resulting in a stiffening mechanism which may be desirable for flatfoot condition to improve stability. This effect seems to be more related to geometry rather than material properties, even though the non-linear contact between keel and heel is affected by the deformation of each single component. The insertion of different wedges in the same region changes the base lever arm length. The interaction between the two components may be used to generate the desired stiffness profile. In the 10° compression trial, the sudden increase in stiffness is noticeable, likely caused by the contact of the heel blade when the CoP travels from toe to midfoot. Presence of the silicon footshell and patient's shoe may filter this effect during prosthetic gait. In fact, the missing footshell represents a limiting factor of the proposed analysis, since the prosthetic foot is typically used in combination with the footshell and, thus, its behavior should be accounted during foot performance analysis. Nonetheless, the goal of this research was to provide a methodological approach to assess the performance of carbon fiber prosthetic feet by means of FEA simulations. These simulations can then be used to optimize the foot design independently from the footshell characteristics, hence decoupling the two components (foot and footshell) contributions to the overall gait performance.

The RoS characterization reproduces the experimental condition despite the simplifying assumption made with respect to the absence of friction. Figure 7 shows that the general shape of the RoS curve is well replicated. The radius error (+10.2%) is caused by the different stiffness of the foot during heel strike, where less deformation produces a bigger radius. Curtze *et al.*[24] investigated the RoS of a Vari-Flex foot (size 27 - CAT unknown) and estimated a RoS radius of 280 mm. However, they implemented a different methodology applying constant weight (about 687 N) throughout the trial, while - in the current study - the heel region has been loaded in a range from around 500 N to 650 N, according to the confidence level of the user to load the prosthesis. Moreover, the foot-shell was not included and the same stiffness categories of prosthesis should be considered for a proper comparison. A non-circular trend is observable at the beginning of the RoS profile (Figure 7). This, in fact, represents the heel strike and weight acceptance phases. This part of the experimental RoS affects the radius calculation, and it can be reasonably cropped out for a better fitting. However, this would in turn neglect the first part of the gait cycle. Major *et al.*[31] proposed a possible solution, suggesting the use of different load profiles to completely describe the patient's gait.

A second relevant aspect of our FEA model is the number of points, i.e. the shank angle values, used to sample the rollover shape trajectory. Due to the implemented fitting algorithm, an equal distribution of RoS points along the entire stance phase needs to be achieved to correctly approximate the experimental curve. This is critical since each point represents an additional simulation. On one hand, it is true that a more complex simulation could be implemented to obtain more sampling points at once. However, this usually ends up with an increased computational time that is not desirable in this phase. Our approach consists of finding the minimum number of configurations required to approximate the experimental curve within an acceptable error. It is also important to underline that the fitting algorithm is affected by the

possibility of offsetting the obtained circular arc towards a specific region if the spatial distribution of the points is not uniform. This issue is important for both experimental and simulated data, but more critical in the first case. It has already been discussed the influence of the heel strike contribution to the RoS radius evaluation. In fact, in the experimental data, the number of points available for a single trial is not necessarily equally distributed along the RoS curve and, thus, the results can be affected by the timing at which the foot is compressed on a specific region (which would produce more sampling points). This emphasizes the need of a standard protocol of testing to avoid such issues. On the other hand, a simulated environment can easily solve the problem by carefully choosing the specific configurations to be tested.

The ISO 22675 describes patient loading profile during gait, and it is profitable to implement these loads during FEA modeling to achieve a standardized and accurate evaluation for design. This strengthens the independence between the patient and the methodology. On the other hand, ISO 10328 load scenarios are mainly focused on the prosthesis strength, which is not dealt in this work due to the lack of detailed information on the material properties, the latter being required to perform accurate analysis throughout specific composite failure criteria.

The *Sensitivity Analysis* enforces the tool advantages in a potential design process, showing the contribution of each component to the overall stiffness. Decreasing E_x of heel component does not produce an equal variation as increasing it by same amount. Variations on the keel component are less evident due to its minor contribution to stiffness during heel compression trials. The $\pm 10\%$ variation of E_x of both components results in a major effect compared to $\pm 20\%$ E_x single component variation. This highlights the non-linearity of the contact imposed by the geometric design.

Conclusion

The FEA-based methodology presented in this paper provides a patient-independent tool that is able to accurately replicate the mechanical behavior of a prosthetic foot. The implementation of the RoS radius (evaluated through FEA) as design value should be used to account for patient perception of the foot. The choice is not only based on previous literature and on patients experience of well-known feet, but it should also consider whether or not the radius is within acceptable values. A standardized evaluation of prosthetic feet behavior is advisable in the future of prosthetic design to increase the device performance, the patient acceptance level and to avoid possible bias based on qualitative approaches. By exploiting simplified boundary conditions and standardized load cases from ISO 22675, the simulation provides results with very limited computational time and therefore it constitutes an efficient method to obtain the aforementioned design parameters. The highlighted features of this tool are particularly useful in early stages of passive prosthetic foot design, since they will strongly reduce time and cost without imposing constraints in terms of possible solutions to explore. Even if the developed methodology has been applied to a well-known ESAR foot, it can be replicated to any other foot geometry or material. Moreover, at the cost of an increased computational time, the methodology can be expanded to include also the foot-shell in a future development. This will introduce additional contact interactions and material non-linearity.

Finite Element Analysis validation has been supported by experimental data in both test bench setup and real use scenario, with a maximum error of +6.1% on stiffness and +10.2% on RoS radius. Furthermore, the performed investigations on a commercial prosthetic foot highlighted important aspects of its design: the relation between stiffness non-linearity and keel/heel contact region shift during stance phase, as well as the heel-strike contribution to the RoS radius value.

Conflict of interest statement

The authors are not in any conflict of interest with regards to the work presented in this paper.

Acknowledgments

This work has been funded by INAIL/Rehab Technologies Laboratory in the Italian Institute of Technology. Support was also provided by Politecnico di Torino. The authors would also like to thank Marco Freddolini, Roberto Capetta, Elisa Catto and Lorenzo Orciari for the support provided during the tests.

References

1. Versluys R, Beyl P, Damme MV, Desomer A, Ham RV, Lefeber D. Prosthetic feet: State-of-the-art review and the importance of mimicking human ankle-foot biomechanics. Disability and Rehabilitation: Assistive Technoloy 2009;4:2:65–75. doi:10.1080/17483100802715092.
2. Fey N, Klute G, Neptune R. Optimization of prosthetic foot stiffness to reduce metabolic cost and intact knee loading during below-knee amputee walking: A theoretical study. Journal of Biomechanical Engineering 2011;134:11:111005. doi:10.1115/1.4007824.
3. Smith K, Gordon A. Mechanical characterization of prosthetic feet and shell covers using a force loading apparatus. Experimental Mechanics 2017;54(4). doi:10.1007/s11340-017-0285-z.
4. Adamczyk P, Roland M, Hahn M. Sensitivity of biomechanical outcomes to independent variations of hindfoot and forefoot stiffness in foot prostheses. Human Movement Science 2017;54:154–71. doi:10.1016/j.humov.2017.04.005.
5. Halsne E, Czerniecki J, Shofer J, Morgenroth D. The effect of prosthetic foot stiffness on foot-ankle biomechanics and relative foot stiffness perception in people with transtibial amputation. Clinical Biomechanics 2020;80. doi:doi.org/10.1016/j.clinbiomech.2020.105141.
6. Klodd E, Hansen A, Fatone S, Edwards M. Effects of prosthetic foot forefoot flexibility on oxygen cost and subjective preference rankings of unilateral transtibial prosthesis users. Journal of Rehabilitation Research & Development 2010;47:6:543–52. doi:10.1682/JRRD.2010.01.0003.
7. Zelik K, et al. . Systematic variation of prosthetic foot spring affects center-of-mass mechanics and metabolic cost during walking. IEEE Transactions on Neural Systems and Rehabilitation Engineering 2011;19:4:411–9. doi:10.1109/TNSRE.2011.2159018.

8. Fey N, Klute G, Neptune R. The influence of energy storage and return foot stiffness on walking mechanics and muscle activity in below-knee amputees. Clinical Biomechanics 2011;26:10:1025–32. doi:10.1016/j.clinbiomech.2011.06.007.
9. Rashke S, Ordendurff M, Mattie J, Kenyon D, Jones O, Moe D, et al. Biomechanical characteristics, patient preference and activity level with different prosthetic feet: A randomized double blind trial with laboratory and community testing. Journal of Biomechanics 2015;48:1:146–52. doi:10.1016/j.jbiomech.2014.10.002.
10. Morgenroth D, Segal A, Zelik K, Czerniecki J, Klute G, Adamczyk P, et al. The effect of prosthetic foot push-off on mechanical loading associated with knee osteoarthritis in lower extremity amputees. Gait & Posture 2011;34:4:502–7. doi:10.1016/j.gaitpost.2011.07.001.
11. Winter D, Sienko S. Biomechanics of below-knee amputee gait. Journal of Biomechanics 1988;21:5:361–7. doi:10.1016/0021-9290(88)90142-X1.
12. Hafner B, Sanders J, Czerniecki J, Fergason J. Transtibial energy-storage-and-return prosthetic devices: a review of energy concepts and a proposed nomenclature. Journal of Rehabilitation Research and Development 2002;39(1):1–11.
13. Hafner B, Sanders J, Czerniecki J, Fergason J. Energy storage and return prostheses: does patient perception correlate with biomechanical analysis? Clinical Biomechanics 2002;17:5:325–44. doi:10.1016/S0268-0033(02)00020-7.
14. Omasta M, Paloušek D, Návrat T, Rosický J. Finite element analysis for the evaluation of the structural behaviour, of a prosthesis for trans-tibial amputees. Medical Engineering and Physics 2012;34:38–45. doi:10.1016/j.medengphy.2011.06.014.
15. Olesnavage K, Winter A. Analysis of rollover shape and energy storage and return in cantilever beam-type prosthetic feet. In: ASME 2014 International Design Engineering Technical Conferences and Computers and Information in Engineering Conference. 2014, p. V05AT08A018. doi:10.1115/DETC2014-35174.
16. Hamzah M, Gatta A. Design of a novel carbon-fiber ankle-foot prosthetic using finite element modeling. IOP Conference Series: Materials Science and Engineering 2018;433:012056. doi:10.1088/1757-899X/433/1/012056.
17. Bonnet X, Helene P, P. F, François L, Wafa S. Finite element modelling of an energy-storing prosthetic foot during the stance phase of transtibial amputee gait. Proceedings of the Institution of Mechanical Engineers Part H, Journal of engineering in medicine 2012;226(14):70–5. doi:10.1177/0954411911429534.
18. Song Y, Choi S, Kim S, Roh J, Park J, Park SH, et al. Performance test for laminated-type prosthetic foot with composite plates. International Journal of Precision Engineering and Manufacturing 2019;20(10):1777–86. doi:10.1007/s12541-019-00156-3.
19. Tryggvason H, Starker F, Lecompte C, Jonsdottir F. Modeling and simulation in the design process of a prosthetic foot. In: Proceedings of the 58th Conference on Simulation and Modelling (SIMS 58). 2017, p. 398–405. doi:10.3384/ecp17138398.
20. Hansen AH, Childress DS, Knox EH. Roll-over shpaes of human locomotor systems: effects of walking speed. Clinical Biomechanics 2003;19(4):407–14. doi:10.1016/j.clinbiomech.2003.12.001.
21. Hansen A, Childress D. Investigations of roll-over shape: implications for design, alignment, and evaluation of ankle-foot prostheses and orthoses. Disability and Rehabilitation 2010;32:26:2201–9. doi:10.3109/09638288.2010.502586.

22. Adamczyk P, Collins S, Kuo A. The advantages of a rolling foot in human walking. The Journal of Experimental Biology 2006;209:3953–63. doi:10.1242/jeb.02455.
23. Adamczyk PG, Kuo AD. Mechanical and energetic consequences of rolling foot shape in human walking. Journal of Experimental Biology 2013;216(14):2722–31. doi:10.1242/jeb.082347.
24. Curtze C, Hof A, van Keeken G, Halbertsma J, Postema K, Otten B. Comparative roll-over analysis of prosthetic feet. Journal of Biomechanics 2009;42:1746–53. doi:10.1016/j.jbiomech.2009.04.009.
25. Ko. C, Kim S, Chang J, Kim Y, Ryu S, Mun M. Comparison of ankle angle adaptations of prosthetic feet with and without adaptive ankle angle during level ground, ramp, and stair ambulations of a transtibial amputee: a pilot study. Clinical Biomechanics 2014;15(12):2689–93. doi:10.1007/s12541-014-0645-x.
26. Ernst M, Altenburg B, Bellmann M, Schmalz T. Standing on slopes - how current microprocessor-controlled prosthetic feet support transtibial and transfemoral amputees in an everyday task. Journal of NeuroEngineering and Rehabilitation 2017;117(14). doi:10.1186/s12984-017-0322-2.
27. Mahmoodi P, Aristodemou S, Ransing R, Owen N, Friswell M. Prosthetic foot design optimisation based on roll-over shape and ground reaction force characteristics. Proceedings of the Institution of Mechanical Engineers, Part C: Journal of Mechanical Engineering Science 2017;231(17):3093–103. doi:10.1177/0954406216643110.
28. Balaramakrishnan TM, Natarajan S, Srinivasan S. Roll-over shape of a prosthetic foot: a finite element evaluation and experimental validation. Med Biol Eng Comput 2020;58(10). doi:10.1007/s11517-020-02214-9.
29. Zhao S, Gabourie R, Faris M, Robertson M, Li Q, Bryant J. Ground reaction force and shank angle waveforms for prosthetic foot mechanical characterization. In: International Society for Prosthetics and Orthotics (ISPO) World Congress. ISPO World Congress; 2015, p. 1.
30. Womac ND, Neptune RR, Klute GK. Stiffness and energy storage characteristics of energy storage and return prosthetic feet. Prosthetics and Orthotics International 2019;43(3):266–75. doi:10.1177/0309364618823127.
31. Major M, Twiste M, Kenney L, Howard D. Amputee independent prosthesis properties–a new model for description and measurement. Journal of Biomechanics 2011;44:2572–5. doi:10.1016/j.jbiomech.2011.07.016.